Pergamon

Cement and Concrete Research 30 (2000) 731–737

CEMENT AND CONCRETE RESEARCH

# Micromechanical modeling of brick-masonry fracture

G.V. Guinea[a,*], G. Hussein[b], M. Elices[a], J. Planas[a]

[a]*Departamento de Ciencia de Materiales, Universidad Politécnica de Madrid, Madrid, Spain*
[b]*Faculty of Engineering, Aim Shams University, El Cairo, Egypt*

Received 18 May 1999; accepted 31 January 2000

**Abstract**

This paper presents a micromechanical model for the analysis of mode I fracture of brick masonry. The analysis is based on a detailed modeling of brick and mortar fracture by means of the fictitious (or cohesive) crack model. Fracture properties for brick and mortar are first independently determined by specific tests and then are input to a numerical model in which bricks and mortar joints are treated separately. The composite fracture model obtained in this way can accurately *predict* the fracture of masonry panels. 

*Keywords:* Masonry; Fracture; Micromechanics; Modeling; Mortar

## 1. Introduction

Brick masonry is an ancient building technique, and masonry structures constitute a large portion of buildings around the world. During decades, the analysis of these structures was based on rules of thumb or empirical formulae, but recently, the research community has begun to show increasing interest in more refined models. The new approaches have partially been promoted by the problem of degradation of historical buildings, where often, a faulty diagnosis brings the restoration process to end by increasing the degradation of masonry. Not less important is the need for more efficient building techniques, especially in the developing and third world countries of Latin America, Asia, and Africa.

Masonry is a composite material made of brick units, usually made from clay, and mortar joints. The large number of variables influencing the mechanical behaviour of masonry, e.g. material properties of brick and mortar, geometry of bricks, joint dimensions, joint arrangement, etc. forced the early analyses to be dramatically simple; masonry was often assumed to be isotropic elastic [1,2]. The development of numerical techniques led to more refined models which separately model bricks and joints, and allow for local failure inside these components [3,4].

Depending on the scale, the modeling of masonry structures can be performed with different levels of abstraction, from a detailed representation of bricks and mortar [5] to a global analysis as an isotropic or orthotropic continuum [6,7]. The grade of refinement is directly related to the problem being analyzed; in large structures a homogeneous material law for the masonry composite seems appropriate to predict deformations and structural displacements at low and medium stress levels, whereas such an approximation can be inadequate when assessing masonry failures. In this case, the stress concentration induces tensile cracks propagating from the existing microdefects in the mortar or at the mortar/brick interface through the mortar beds, debonding or breaking the bricks. The stress redistribution is then directly influenced by the inhomogeneity of the material at the meso-scale level, and the load and the displacements are controlled by the way brick and mortar interact [2]. For these situations, a detailed modeling can bring more accurate predictions. This is also the case when the masonry structure contains no more than a few units, and a continuous modeling is no longer valid.

This paper presents a micromechanical model for the analysis of mode I fracture of brick masonry. The analysis is based on a detailed modeling of brick and mortar fracture by means of the fictitious crack model [8], which has shown its utility in modeling the fracture process in concrete and

* Corresponding author. Departamento de Ciencia de Materiales, E.T.S.I. Caminos, Ciudad Universitaria s/n, 28040 Madrid, Spain. Tel.: +34-91-336-64-29; fax: +34-91-336-66-80.

*E-mail address*: gguinea@mater.upm.es (G.V. Guinea).

0008-8846/00/$ – see front matter 
PII: S0008-8846(00)00228-3

concrete-like materials when the failure mode is governed by a single macrocrack [8–10]. With this model as a framework, fracture properties of brick and mortar are independently determined by specific tests performed on these materials, and then are input to a numerical simulation where bricks and mortar joints are treated separately. The result is a composite fracture model, which can *predict* the behaviour of the masonry composite without resort to any kind of fitting or tuning procedure.

To check the model, a series of fracture tests was performed on small masonry panels under three-point bending. As will be shown later, the model can accurately predict loads and displacements all over the test records.

The work presented here is not intended to be a small-scale modeling of real masonry walls. With this paper, the authors only want to emphasize that with this new approach, based on a separate modeling of the units and the cementing matrix, it is possible to analyze the fracture behaviour of this kind of composite material. Further work must be done to extend this modeling to full-scale masonry structures.

The following section describes the materials used in this work and the tests performed. Section 3 presents the fracture model and its numerical implementation. Finally, the results from the model and from the experiments are compared in Section 4, which closes the paper.

## 2. Materials and tests

### 2.1. Materials and specimens

To capture the essentials of masonry behaviour while maintaining a reasonable experimental cost, a small-scale model was selected. This methodology, alternative to full-scale testing, has been widely used in masonry research since the mid-'50s, and is helpful in understanding the interaction between bricks and mortar joints [11]. A scale factor of 1/4 was chosen to avoid difficulties in modeling the joint thickness, and to have a representative number of brick units in masonry specimens. Only geometric similitude requirements were considered, and the micro-mortar and the solid brick units used in this work were not intended to represent a real mortar, nor real brick units, as explained before.

Table 1
Mix proportions by weight of the model mortar

| Cement | Sand | Silica fume | Water |
|---|---|---|---|
| 1 | 1.3 | 0.1 | 0.3 |

Small-scale bricks of 48 × 10 × 25 mm$^3$ were cut with a diamond saw from 235 × 40 × 110 mm$^3$ full-scale solid units made from clay. All the units were from the same batch to ensure homogeneous behaviour. Specimen faces were ground during specimen preparation to guarantee planar surfaces.

In addition to these small-scale units, cubes 33 mm in height were sawn for compression and splitting tests, and three sizes of prismatic specimens for fracture tests were produced. These were standard notched beams of 16, 24, and 32 mm depth, with span to depth ratio of 4 and notch to depth ratio of 0.5. All the notches were 0.3 mm wide. Other details can be found elsewhere [12].

The mortar used for masonry panels was designed to meet similitude requirements and to assure a workable mix. A maximum aggregate size of 0.85 mm was selected to be compatible with the scaled-down thickness of the joints of 3 mm. The grading, shown in Fig. 1, complied with ASTM-C-144 standard requirements for masonry mortar, but with the particles removed whose size exceeded No. 16 sieve (1.18 mm). An ordinary Portland cement (ASTM, Type I) was used. To improve the mechanical performance of the mortar, 10% of Silica fume was incorporated. Table 1 gives the proportions of the model mortar.

Prismatic specimens of 480 × 40 × 40 mm$^3$ were cast to characterize the mortar. The cast and curing processes are detailed in Ref. [12].

Two masonry panels were constructed with the mortar and the small-scale units described above. Fig. 2 shows their dimensions. Nine courses of 10 units each were used on average to build a panel. The thickness was kept

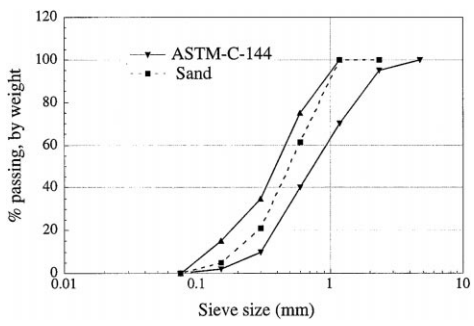


Fig. 1. Grading of mortar.

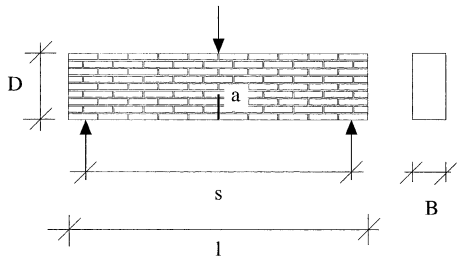


| Beam | a(mm) | D(mm) | s(mm) | l(mm) | B(mm) |
|---|---|---|---|---|---|
| P-3 | 39 | 111.3 | 460 | 521 | 25 |
| P-4 | 39 | 112 | 460 | 523 | 25 |

Fig. 2. Geometry of masonry panels.

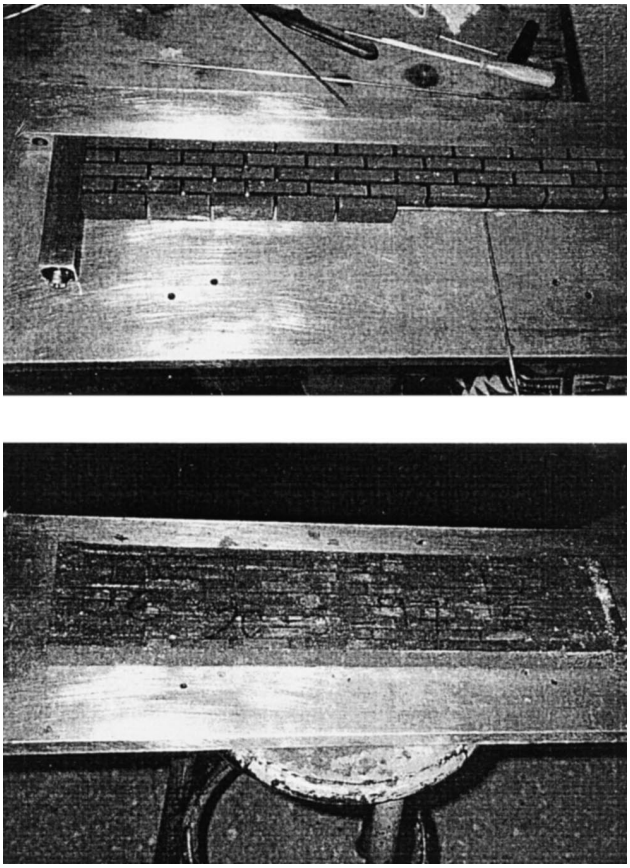

Fig. 3. Fabrication of masonry panels.

constant, equal to that of a unit (25 mm). Fig. 3 shows two stages of the manufacture. First, the bricks were carefully placed on site with the aid of 3-mm diameter spacers. Then, the mortar was poured into the joints and vibrated 10 s. Once the panels were constructed, they were stored 24 h in a water-saturated room. After demolding, the specimens were cured in water at 20°C until testing time. Prior to testing, a central notch 0.3-mm wide was sawn up to 30% of the panel depth.

### 2.2. Tests

Three different characterization tests were performed on mortar and brick components: compressive strength, splitting strength, and fracture under three-point bending.

Table 2
Compressive and splitting strength of brick and mortar

| Material | Compressive strength, $f_c$ (MPa) | Splitting strength, $f_{st}$ (MPa) |
|---|---|---|
| Brick | 76.6 ± 1.5 (15) | 4.66 ± 0.19 (8) |
| Mortar | 58.9 ± 1.9 (7) | 3.32 ± 0.16 (5) |

Mean values and standard deviations are indicated.
Values in parentheses show the number of tests.

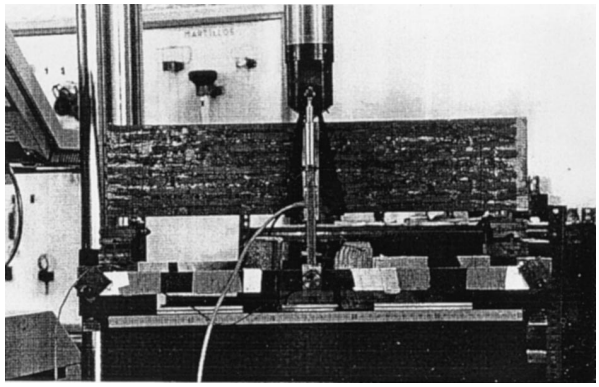

Fig. 4. Three-point bending test of masonry panels.

The test specimens for compressive and splitting-tensile strength were cubes 33 mm in height for the brick and 40 mm for the mortar. Mortar specimens were cut from the precast beams mentioned earlier. All the specimen faces were ground to ensure proper loading. The compression test followed ASTM-C-109 and ASTM-C-67 standards for mortar and brick specimens respectively, with the only exception of specimen size. For splitting tests, the ISO 4108 standard was used. Table 2 summarizes the results.

Three-point bending fracture tests were performed on mortar, brick, and masonry following the RILEM TC-50-FCM recommendation [13] with some improvements by the authors [14–16]. During the test, load–point displacement and crack mouth opening displacement (CMOD) were continuously recorded. Fig. 4 shows the test arrangement for a masonry panel, and Figs. 5 and 6 display the load–displacement curves recorded for brick and mortar specimens.

## 3. Fracture model

The failure analysis of masonry has been based mostly on modeling techniques developed for concrete. Several linear and non-linear fracture theories have been proposed when the failure is governed by the development of a single

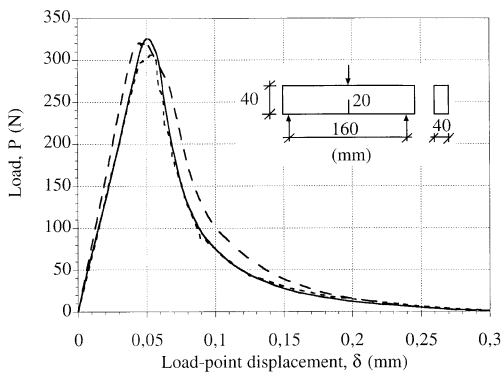


Fig. 5. Three-point bending test of mortar beams.

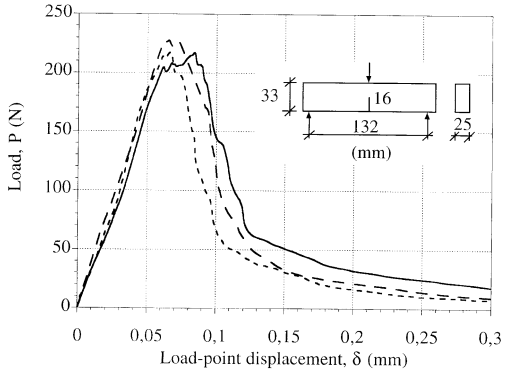


Fig. 6. Three-point bending test of brick beams.

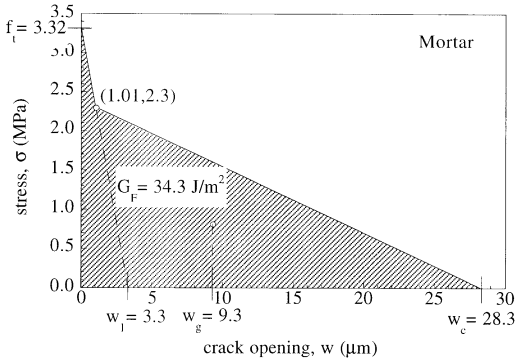


Fig. 8. Softening function for the mortar.

macrocrack, one of the most promising being the cohesive- or fictitious-crack model which gives a suitable macroscopic modeling of the non-linear fracture processes. First introduced by Hillerborg et al. [8] in 1976, it has been successfully used to explain many experimental results in concrete, ceramics, and rocks. The basic properties of a cohesive crack are reviewed in Refs. [9,10]. Previous results reported by some authors suggest that this model can be satisfactorily applied to bricks [17].

The cohesive crack model introduces the softening function to simulate the microcracking and deterioration of the material in the fracture process zone. This zone is modeled by means of a cohesive crack, which can transfer stress—the cohesive stress—from one face to the other. For the simplest configuration, where a crack opens monotonically loaded in mode I, the cohesive stress at a given point σ is normal to the crack faces and is uniquely given by the softening curve as a function of the crack opening at this point $w$, $\sigma = f(w)$, as shown in Fig. 7. The softening function relates the stress transferred between the crack faces to the crack opening at this point, and it is considered by hypothesis to be a material property, independent of geometry and size.

The stress at the tip of the cohesive crack is equal to the tensile strength of the material, $f_t$, and decreases progressively as the crack opening increases. When the crack opening reaches the critical crack opening $w_c$, the cohesive stress drops to zero and a *true*—stress-free—crack propagates. The work done to produce a unit area of true crack is the fracture energy, $G_F$, and coincides with the area under the softening curve.

To simplify the computations, the bulk behaviour is commonly assumed to be linear–elastic, although this approximation can be relaxed if necessary.

### 3.1. Fracture model for mortar and brick

Using the procedure proposed by the authors [16,18], a bilinear softening function was determined from the results of stable three-point bend tests and from the splitting tests. The function and its main parameters for the mortar are given in Fig. 8.

With the same procedure, a linear softening function was determined for the brick. The function is given in Fig. 9. In this case, a linear softening function is enough to model the fracture of brick, as indicated by other authors [17].

### 3.2. Composite model

Once the two components of masonry, mortar, and brick, were modeled by means of the fictitious crack model, they were combined to model the fracture behaviour of the composite. To do this, a detailed modeling of the masonry structure was needed.

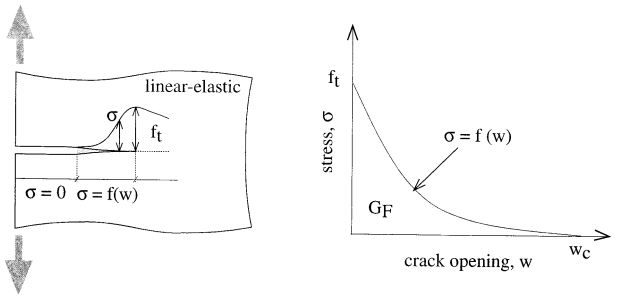


Fig. 7. Cohesive crack and softening function.

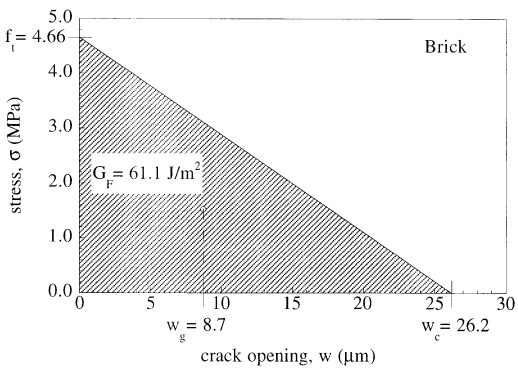


Fig. 9. Softening function for the brick.

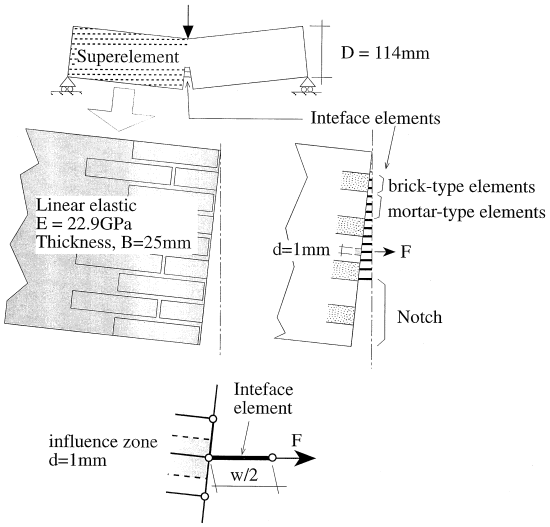


Fig. 10. Modeling with interface elements.

In this work, only mode I fracture of masonry panels under three-point bending was considered. The geometry of the panels was already shown in Fig. 2. For the numerical model, ideal 3 mm-width joints and 10 mm-depth bricks were assumed, giving a total depth of 114 mm. The small difference, less than 3%, from the actual depth of the experimental panels (111 mm) was neglected in the modeling.

Interface elements were placed along the crack path, simulating the properties of the constituent materials, as sketched in Fig. 10. These elements were one-dimensional, with a non-linear force-displacement behaviour. The interface elements were attached to the nodes of the two-dimensional finite element mesh. The force, $F$, acting upon each interface element was that corresponding to the cohesive stresses acting between two adjacent nodes — the "influence zone" of the interface element. Given the symmetry, only a half of the panel was modeled.

The force–deflection curves for the interface elements were determined from the cohesive softening function for each material. The softening curves, $\sigma-w$, were transformed into the force–deflection, $F-w/2$, curves by assigning to the interface element the force corresponding to its influence

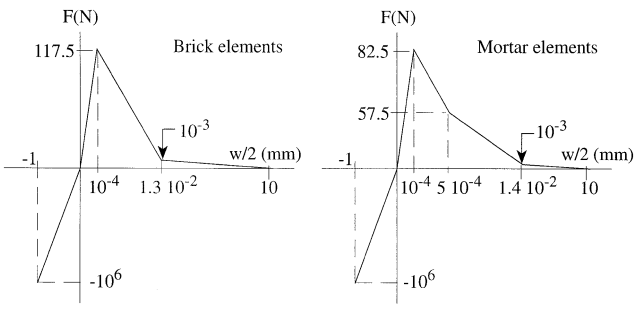


Fig. 11. Force–deflection curves for the interface elements (not to scale).

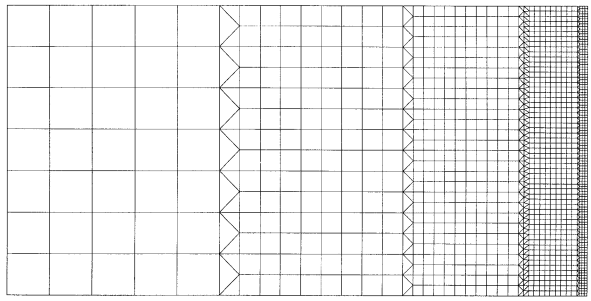

Fig. 12. Finite element mesh for the panel.

zone, as depicted in Fig. 10. A uniform mesh with 114 elements along the crack path was used, hence, the width of the influence zone, $d$, is equal to 1 mm. The resulting force–deflection curves for brick and mortar are presented in Fig. 11. A very stiff initial behaviour in tension and compression was introduced to enhance the convergence while maintaining the precision of computations. For the same reason, a very small (negligible) linear segment was inserted behind the actual softening curve, hence, avoiding zero stiffness in the fully broken elements.

The numerical problem was solved with the commercial finite element code ANSYS® using the substructuring technique to reduce the number of degrees of freedom. A homogeneous linear–elastic behaviour was assumed for all the elements outside the fracture line, with an average elastic modulus of 22.9 MPa. This value was obtained from a fit of the initial linear part of the test records before the cracking started.

Finite elements in the panel were condensed in a super element that was connected to the interface elements. This method is highly recommended in a general non-linear analysis where a portion of the model remains linear–elastic.

The finite element mesh used for the super element is shown in Fig. 12. It was formed by three-node triangular and four-node quadrilateral isoparametric elements. A plane stress state with Poisson's ratio of 0.2 was assumed in the computations. Nodal points along the crack path were

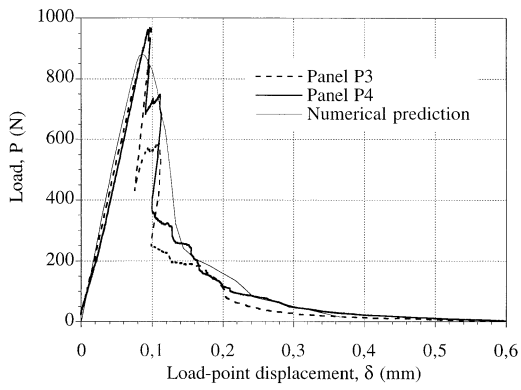


Fig. 13. Load–displacement curves and numerical prediction for masonry panels under three-point bending.

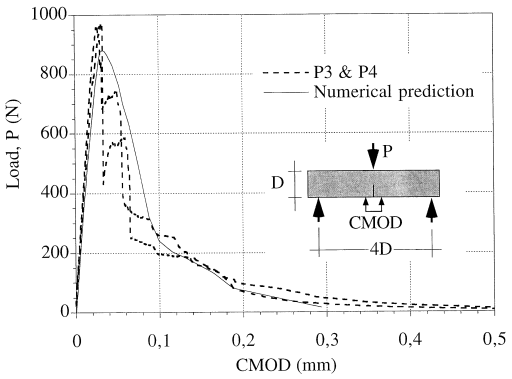


Fig. 14. Load–CMOD curves and numerical prediction for masonry panels under three-point bending.

connected to the interface elements except in the initial notch zone.

## 4. Results and discussion

Figs. 13 and 14 show the load–displacement and load–CMOD curves from the three-point bending tests of masonry, and Table 3 gives the fracture energy, $G_F$, and the modulus of elasticity, $E$. Fracture energy was determined by the work of fracture method as recommended by RILEM, with special care to eliminate any spurious energy consumption apart from the fracture process. The modulus of elasticity was determined from the initial load–CMOD compliance.

Tests were stable due to the CMOD control performed during the experiments. Some minor instabilities in the post peak zone were produced by the sudden break of brick units. The crack propagated through the panel depth from the notch towards the central loading point, breaking the panel in two halves at the end of test. In the load–displacement diagram, the panels presented a snap-back instability, as displayed in Fig. 13.

Comparison of numerical and experimental results in Figs. 13 and 14 reveals that the detailed fracture model presented in this paper can accurately *predict* the experimental records, especially when the load–CMOD curve is considered. Since the load–deflection curve, in opposition to the load–CMOD curve, is very sensitive to the detailed contact between the specimen and the supports [19], which is poorly known, the initial compliance of the load–displacement curves have been fitted "ad-hoc". This is not the case with other displacements not under the loading points, such as the CMOD, which justifies using the load–CMOD curve to check the model. As mentioned earlier, this model is based on the properties of brick and mortar measured by independent tests, and in its present form can be applied to any masonry structure subjected to mode I cracking.

Table 3
Fracture energy and modulus of elasticity of masonry panels

| Fracture energy, $G_F$ (J/m$^2$) | Modulus of elasticity, $E$ (GPa) |
|---|---|
| 45.5 ± 2.7 | 22.9 ± 1.4 |

Mean values and half-range are indicated.

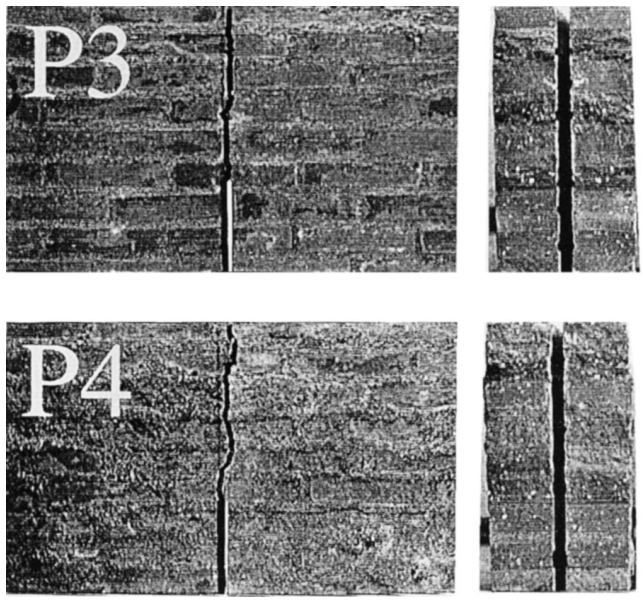


Fig. 15. P3 and P4 specimens after testing.

A good approximation is also achieved if the fracture energy of the masonry panels is estimated from the work of fracture of the constituents, brick, and mortar. The estimated work of fracture is obtained by multiplying the broken area of each material by its corresponding fracture energy. The fracture energy of masonry computed in this way is 44.8 J/m$^2$, close to the 45.5 J/m$^2$ measured in the tests.

It is important to note that the model presented in this paper does not consider distributed cracking or damage in the structure, and applies only when a macrocrack develops. Fig. 15 shows the failed specimens where a single dominant crack is observed that runs vertically through the mortar beds and the brick units. This fact restricts its practical application to relatively large masonry structures, such as masonry walls. For medium or small masonry panels, a more detailed analysis of brick and mortar interaction would be required.

## Acknowledgments

The authors gratefully acknowledge the support, for this research, provided by the Spanish Comisión Interministerial de Ciencia y Tecnología (CICYT), under grants MAT97-1022 and MAT97-1007-C02-02.

## References

[1] R.H. Wood, Studies in composite construction part 1. The composite action of brick panel walls supported on reinforced concrete beams,

Research Paper No. 13, National Building Studies, Building Research Station, Waterford, UK, 1952.
[2] S. Rosenhaupt, Y. Sokoal, Masonry walls on continuous beams, J Struct Div, Am Soc Civ Eng 91 (1) (1965) 155–171.
[3] S. Ali, A.W. Page, Finite element model for masonry subjected to concentrated loads, J Struct Div, Am Soc Civ Eng 114 (8) (1988) 1761–1784.
[4] P.B. Lourenco, J.G. Rots, Multisurface interface model for analysis of masonry structures, J Eng Mech Div, Am Soc Civ Eng 123 (7) (1997) 660–668.
[5] J.G. Rots, Numerical simulation of cracking in structural masonry, Heron 36 (2) (1991) 49–63.
[6] M. Dhanasekar, P.W. Kleeman, A.W. Page, Biaxial stress–strain relations for brick masonry, J Struct Div, Am Soc Civ Eng 111 (5) (1985) 1085–1100.
[7] H.R. Lofti, P.B. Shing, An appraisal of smeared crack models for masonry shear wall analysis, Comput Struct 41 (3) (1991) 413–425.
[8] A. Hillerborg, M. Modeer, P.E. Petersson, Analysis of crack formation and crack growth in concrete by means of fracture mechanics and finite elements, Cem Concr Res 6 (1976) 773–782.
[9] M. Elices, J. Planas, Material models, in: L. Elfgren (Ed.), Fracture Mechanics of Concrete Structures, Chapman & Hall, London, (1989) 16–66, Chap. 3.
[10] M. Elices, J. Planas, G.V. Guinea, Modeling cracking in rocks and cementitious materials, in: H.P. Rosmanith (Ed.), Fracture and Damage of Concrete and Rock, E&FN Spoon, London, (1993) 3–33.
[11] B.E. Abboud, A.A. Hamid, H.G. Harris, Small-scale modeling of concrete block masonry structures, ACI Struct J 87 (2) (1990) 145–155.
[12] G. Hussein, Application of Fracture Mechanics to Masonry Cracking, PhD dissertation, Universidad Politécnica de Madrid (in Spanish), 1997.
[13] RILEM TC 50 FCM Draft Recommendation, Determination of the fracture energy of mortar and concrete by means of three-point bend tests on notched beams, Mater Struct 18 (106) (1985) 285–290.
[14] G.V. Guinea, J. Planas, M. Elices, Measurement of the fracture energy using three-point bend tests: 1. Influence of experimental procedures, Mater Struct 25 (1992) 212–218.
[15] J. Planas, M. Elices, G.V. Guinea, Measurement of the fracture energy using three-point bend tests: 2. Influence of bulk energy dissipation, Mater Struct 25 (1992) 305–312.
[16] M. Elices, G.V. Guinea, J. Planas, Measurement of the fracture energy using three-point bend tests: 3. Influence of cutting the $P-\delta$ tail, Mater Struct 25 (1992) 327–334.
[17] P. Bocca, A. Carpinteri, S. Valente, Fracture analysis of brick masonry: Size effects and snap-back analysis, Mater Struct 22 (1989) 364–373.
[18] G.V. Guinea, J. Planas, M. Elices, A general bilinear fit for the softening curve of concrete, Mater Struct 27 (1994) 99–105.
[19] J. Planas, G.V. Guinea, M. Elices, Stiffness associated with quasi-concentrated loads, Mater Struct 27 (1994) 311–318.